NeuroImage 60 (2012) 1307–1315

Contents lists available at SciVerse ScienceDirect

NeuroImage

journal homepage: www.elsevier.com/locate/ynimg

Abnormal cortical processing of pattern motion in amblyopia: Evidence from fMRI

B. Thompson [a,b,*], M.Y. Villeneuve [c,d], C. Casanova [e], R.F. Hess [b]

[a] Department of Optometry and Vision Science, University of Auckland, Private Bag 92019, Auckland, New Zealand
[b] McGill Vision Research, Department of Ophthalmology, McGill University, Royal Victoria Hospital, 687 Pine Avenue West, Montreal, Canada
[c] NMR Martinos Center, Massachusetts General Hospital, Harvard Medical School, Harvard University, Boston, USA
[d] Montreal Neurological Institute, Departments of Neurology and Neurosurgery, McGill University, Montreal, Canada
[e] Laboratoire des Neurosciences de la Vision, École d'optométrie, Université de Montréal, CP 6128, succ. Centre-Ville, Montreal, Canada

ARTICLE INFO

Article history:
Received 12 November 2011
Revised 29 December 2011
Accepted 14 January 2012
Available online 24 January 2012

Keywords:
Amblyopia
Motion
MT+
V5
Plaid
Dorsal Stream

ABSTRACT

Converging evidence from human psychophysics and animal neurophysiology indicates that amblyopia is associated with abnormal function of area MT, a motion sensitive region of the extrastriate visual cortex. In this context, the recent finding that amblyopic eyes mediate normal perception of dynamic plaid stimuli was surprising, as neural processing and perception of plaids has been closely linked to MT function. One intriguing potential explanation for this discrepancy is that the amblyopic eye recruits alternative visual brain areas to support plaid perception. This is the hypothesis that we tested. We used functional magnetic resonance imaging (fMRI) to measure the response of the amblyopic visual cortex and thalamus to incoherent and coherent motion of plaid stimuli that were perceived normally by the amblyopic eye. We found a different pattern of responses within the visual cortex when plaids were viewed by amblyopic as opposed to non-amblyopic eyes. The non-amblyopic eyes of amblyopes and control eyes differentially activated the hMT+ complex when viewing incoherent vs. coherent plaid motion, consistent with the notion that this region is centrally involved in plaid perception. However, for amblyopic eye viewing, hMT+ activation did not vary reliably with motion type. In a sub-set of our participants with amblyopia we were able to localize MT and MST within the larger hMT+ complex and found a lack of plaid motion selectivity in both sub-regions. The response of the pulvinar and ventral V3 to plaid stimuli also differed under amblyopic vs. non-amblyopic eye viewing conditions, however the response of these areas did vary according to motion type. These results indicate that while the perception of the plaid stimuli was constant for both amblyopic and non-amblyopic viewing, the network of neural areas that supported this perception was different.

Introduction

Amblyopia is a developmental disorder of the visual system characterized by reduced vision in an otherwise healthy eye. The condition occurs when each eye sees a different image during infancy, typically due to the presence of chronic blur in one eye (anisometropia), a misalignment of the visual axes (strabismus) or visual deprivation. Under these conditions, the visual system may develop so that the inputs from the eye with the weaker or suppressed image are processed abnormally within the visual cortex (Hubel and Wiesel, 1965, 1970; Kiorpes and McKee, 1999). This impoverished early visual experience can impair both spatial and temporal vision (Asper et al., 2000; Barrett et al., 2004) and the effects appear to extend to extrastriate visual areas (Barnes et al., 2001; Bonhomme et al., 2006; Hess et al., 2010; Li et al., 2011).

There is increasing evidence that amblyopia is associated with abnormal function of a specific region of the dorsal extrastriate processing stream known as area MT. This region is highly motion sensitive and contains cells that can integrate local motion signals into a coherent motion representation (Born and Bradley, 2005; Majaj et al., 2007; Movshon et al., 1985). Evidence for an MT deficit in humans with amblyopia comes primarily from psychophysical studies of global motion perception using random dot kinematograms (RDKs) as stimuli. These stimuli consist of two populations of moving dots; a population of "signal dots" which have a common motion direction and a population of "noise dots" which move randomly. The observer's task is to identify the direction of the signal dots. This requires the integration of coherent local motion signals and the segregation of these coherent signals from noise. There is strong neurophysiological evidence to suggest that this process involves area MT. For example, lesions of MT selectively impair perception of RDKs (Newsome and Pare, 1988) and microstimulation of MT can influence perceptual judgments of RDK motion (Salzman et al., 1990). Therefore, the large number of psychophysical studies that have demonstrated abnormal perception of global motion in amblyopia, even when deficits in

* Corresponding author at: Department of Optometry and Vision Science, University of Auckland, Private Bag 92019, Auckland 1142, New Zealand. Fax: +64 9 373 7058.
E-mail address: b.thompson@auckland.ac.nz (B. Thompson).

1053-8119/$ – see front matter © 2012 Elsevier Inc. All rights reserved.
doi:10.1016/j.neuroimage.2012.01.078

contrast sensitivity are accounted for, strongly suggests that MT is affected by this disorder (Aaen-Stockdale and Hess, 2008; Aaen-Stockdale et al., 2007; Constantinescu et al., 2005; Ellemberg et al., 2002; Ho and Giaschi, 2009; Ho et al., 2005; Mansouri and Hess, 2006; Simmers et al., 2003, 2006).

A different visual stimulus that has been used extensively to investigate the neural mechanisms supporting motion integration and segregation is the plaid. Plaid stimuli are typically constructed from two gratings drifting in different directions within a circular aperture. If the spatial and temporal properties of the two gratings are sufficiently similar to one another, the gratings will cohere and produce the percept of a single patterned surface drifting in a direction that can be unique from either component direction, known as pattern or coherent motion (Adelson and Movshon, 1982). However, if the gratings differ sufficiently in their spatial or temporal properties they will not cohere, but rather will appear to drift over one another, generating a transparent percept known as component or incoherent motion (Adelson and Movshon, 1982; Smith, 1992). A subset of cells in MT has been shown to encode the coherent or "pattern" motion of plaid stimuli (Movshon et al., 1985; Pack et al., 2001; Rodman and Albright, 1989; Stoner and Albright, 1992). In addition, the perception of coherent plaid motion has been linked to MT function in humans. For example Huk and Heeger (2002) used an fMRI adaptation paradigm to demonstrate that the hMT+ complex (which includes both MT and MST homologs) had a strong selectivity for coherent plaid motion. In agreement with these findings, Castelo-Branco et al. (2002), also using fMRI, demonstrated that activity in hMT+ was correlated with perceptual switches between coherent and incoherent motion for bi-stable plaid stimuli. These authors also reported stronger activation in hMT+, as well as other extrastriate areas, for incoherent vs. coherent motion. This may be explained by incoherent motion activating two motion direction selective neural assemblies, with coherent motion activating only one pattern motion selective neural assembly. Evidence for the link between hMT+ and plaid perception has also been found from lesion studies, whereby lesions affecting hMT+ reduce coherent motion perception (Clifford and Vaina, 1999). This finding is supported by a recent study in which coherent perception of plaids was altered by temporary disruption of processing in hMT+ using repetitive transcranial magnetic stimulation (Thompson et al., 2009).

In the light of the previous work indicating an MT deficit in amblyopia, we conducted a psychophysical experiment investigating the ability of amblyopic eyes to perceive coherent and incoherent plaid stimuli (Thompson et al., 2008). Our hypothesis was that abnormal processing in MT would produce a preponderance of incoherent motion percepts for amblyopic eye viewing. To our surprise, however, we found that amblyopic eyes mediated largely normal perception of both coherent and incoherent plaids. There are at least two possible explanations for this finding. The first is that the integration of local motion signals in MT is abnormally susceptible to noise in amblyopia, and it is the presence of noise in the RDK stimuli rather than a motion integration deficit per se that causes the impaired performance (Mansouri and Hess, 2006). The second explanation is that an alternative network of neural areas is recruited to support normal plaid perception by the amblyopic eye. Candidate areas include those that have been shown to possess cells with selectivity for coherent plaid motion, and include V1 (Guo et al., 2004), V3 (Gegenfurtner et al., 1997; Wenderoth et al., 1999) and the pulvinar (Merabet et al., 1998; Villeneuve et al., 2005). These two explanations are not mutually exclusive. It is conceivable that if an alternative neural network underpins complex motion perception for amblyopic viewing, this network may be more susceptible to noise than the presumably optimal network recruited by non-amblyopic eyes.

This study was designed to test the hypothesis that normal perception of plaid stimuli by amblyopic eyes is mediated by a network of visual areas that is distinct from those recruited by non-amblyopic eyes. We used functional magnetic resonance imaging (fMRI) to measure the response of the amblyopic visual cortex and pulvinar to plaid stimuli that generated consistent percepts of coherent or incoherent motion for both amblyopic and non-amblyopic eyes. We found that, contrary to control eye and non-amblyopic-eye viewing, the hMT+ complex was not differentially activated by coherent vs. incoherent motion when stimuli were viewed with an amblyopic eye. This suggests that alternative visual areas may support plaid perception by the amblyopic eye. Our data allowed for the tentative identification of ventral V3 and the pulvinar as two candidate areas that may be differentially involved in motion processing under amblyopic eye viewing conditions.

Methods

Participants

Six adults with amblyopia and seven control observers (6 males, average age 31.1 years) took part in this study. All observers with amblyopia had a strabismus and two also had anisometropia. Clinical details for the observers with amblyopia are provided in Table 1. All participants gave informed consent prior to participating in this study and all study protocols were approved by the institutional ethics committee and were in accordance with the declaration of Helsinki.

Stimuli

Plaids

During scanning, participants viewed plaid stimuli constructed from two superimposed drifting sine wave gratings of 50% contrast that differed in their orientation by 120° (one grating oriented 60° right of vertical and the other 60° left of vertical). Three dynamic plaid patterns were presented during scanning (Fig. 1). Two plaids

Table 1
Clinical details of the observers with amblyopia. Obs = observer, LA=letter acuity, M = male, F = female, RE = right eye, LE = left eye, strab = strabismus, DS = dioptre sphere, XT = exotopia, ET = esotropia, y = years of age, m = months.

Obs	Age/sex	Type	Refraction	LA	Squint	History, stereo
AR	48/M	RE	Ø	20/20		Detected age 6 y, no patching, no surgery.
		LE strab	Ø	20/50	XT 1°	
AS	22/F	RE	Ø	20/20		Detected age 4 y, patching at 4 y for 6 m, surgery at 7 y.
		LE strab	−0.5DS	20/160	ET 15°	
GN	31/M	RE mixed	+5.00–2.00×120°	20/70	ET 8°	Detected age 2 y, strabismus surgery ages 2–6 y.
		LE	+3.50–1.00×75°	20/20		
ML	21/F	RE mixed	+1.0–0.75	20/80	ET 6°	Detected age 5 y, patching for 2 y, no surgery.
		LE	-3.25	20/25		
RD	50/M	RE	+3.00DS	20/15		Detected age 6 y, glasses 6 y, no patching, no surgery.
		LE strab	+4.00DS	20/125	ET 1°	
VD	24/F	RE	+0.25DS	20/20		Detected age 5–6 y, patching for 6 m, no surgery.
		LE mixed	+2.75–1.25×175°	20/40	ET3°	

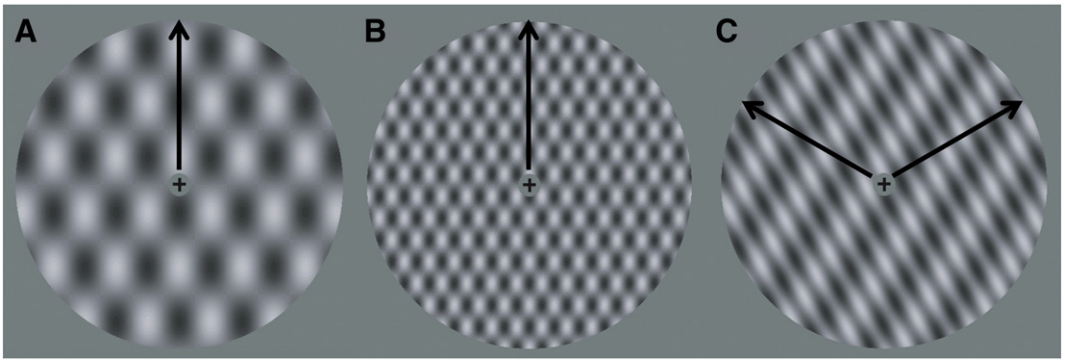

Fig. 1. The plaid stimuli presented during scanning. A and B represent the two coherent plaids constructed from 0.2 cpd and 0.5 cpd components respectively. C represents the incoherent plaid constructed from one 0.2 cpd and one 0.5 cpd component. The arrows represent the perceived motion direction(s) for illustrative purposes only and were not present in the actual stimuli.

were constructed from component gratings with identical spatial frequencies; one plaid with 0.2 cpd components referred to as the low spatial frequency (LSF) plaid, (Fig. 1A) and one with 0.5 cpd components referred to as the high spatial frequency (HSF) plaid, (Fig. 1B). The final, incoherent, plaid was constructed from a 0.2 cpd component and a 0.5 cpd component grating (Fig. 1C). Plaids were presented within a 30° circular aperture and the component gratings had a temporal frequency of 4 Hz. The two plaids with identical spatial frequency components gave rise to a robust percept of coherent motion whereas the plaid with the components that differed in their spatial frequency produced a robust incoherent motion percept. A fourth stationary plaid pattern constructed from two 0.2 cpd components was also included during scanning. The central 2° of each plaid pattern was blanked out to allow for steady fixation without the induction of optokinetic nystagmus. A central fixation cross was provided within this blanked out region.

Scans were performed monocularly with a tight fitting eyepatch covering the non-viewing eye. During scanning, plaids were presented continuously for 16 s. Each 16 second block of plaid presentation was followed by a 16 second block of mean luminance blank fixation. Each of the four plaid stimuli (three dynamic plaids and one static plaid) was presented twice within each scan and each session contained six plaid stimulus scans. This provided for three monocular scans per eye for the observers with amblyopia and three scans under dominant eye monocular viewing conditions for controls. Controls also completed three scans under binocular viewing conditions for use in a different study and these data are not included in this paper. Non-dominant eye data were not collected for controls as we did not anticipate any interocular differences for these participants with normal binocular vision. During scanning participants continually reported their plaid percept by holding down one button on the response box if they perceived coherent motion and a different button if they perceived incoherent motion (Hupe and Rubin, 2003; Thompson et al., 2008). This allowed for participants to report a switch in percept during a block by changing response buttons. Participants were not required to make behavioral responses during static plaid blocks or during blank fixation.

Localization and subdivision of hMT+

Differences in the representation of the visual field within MT and MST were used to sub-divide hMT+ into MT and MST (Dukelow et al., 2001; Huk et al., 2002; Smith et al., 2006). Specifically, cells in area MT have receptive fields that are primarily responsive to the contralateral hemifield while area MST contains larger receptive fields that also respond to stimuli presented within the ipsilateral visual field. In fact, neurons in macaque area MST can encode up to 40° of the ipsilateral visual field (Desimone and Ungerleider, 1986; Duffy and Wurtz, 1991; Komatsu and Wurtz, 1988; Raiguel et al., 1997). We used a large RDK to localize hMT+ and subdivided this region into MT and MST following previously reported protocols (Dukelow et al., 2001; Huk et al., 2002; Smith et al., 2006). The stimulus consisted of white dots (1° in diameter, 0.2 dots/deg^2) on a black background presented within a 40° circular aperture. During scanning the stimulus was presented in four different states; full field motion, left hemifield motion, right hemifield motion and static. During full field motion all stimulus dots underwent sequential centripetal and centrifugal motion (expansion and contraction) at a speed of 8°/s. For hemifield stimulation, the RDK remained static with the exception of a 10° circular region centered 15° horizontally from fixation which underwent centripetal and centrifugal motion. In each hemisphere, the contrast between full field motion and static dots was used to identify hMT+. MST was then defined as the region within the hMT+ complex that responded to ipsilateral hemi-field stimulation. Finally, MT was identified as the region within hMT+ responsive to contralateral hemifield stimulation after MST had been removed. During scanning, the four stimulus conditions were presented for 16 s and were separated by 16 second blocks of blank fixation (blank screen). Each condition was repeated twice per scan. During scanning, participants were required to maintain fixation on a cross in the center of the display and press a response button whenever they detected a reversal in motion direction. Participants were not required to make behavioral responses during static or fixation blocks. There were four monocular scans (two per eye) for the observers with amblyopia and two monocular dominant eye scans and two binocular viewing scans for controls.

Retinotopic mapping

Standard retinotopic mapping protocols were used with visual stimuli, and protocols identical to those described previously (Barnes et al., 2010; Li et al., 2007). Retinotopic wedge and annulus checkerboard sections, conventionally used for retinotopic mapping, were presented in a phase-encoded sequence while the participant attended to a central fixation cross. The subjects also performed a visual task designed to control for attention which required the detection of a coherent patch of checkerboard within the checkerboard stimulus as a whole that appeared at random times and positions.

Stimulus presentation

Stimuli were back projected onto a screen mounted at the head end of the scanner bore using an NEC 820 LDC video projector (1024×768 pixel resolution, 60 Hz refresh rate). The projection screen was viewed by the participant by means of an angled mirror mounted above their eyes. During scanning fixation was monitored using an MRI compatible infrared video camera connected to custom eye tracking software. Participants viewed the stimuli monocularly with a tight-fitting eyepatch occluding one eye. The viewing eye was alternated scan by scan for the participants with amblyopia and the eye tracking system was adjusted accordingly. Control participants viewed the stimuli with their

dominant eye only. Participants wore their full refractive correction during scanning.

Procedure

Participants took part in two separate scanning sessions, one for retinotopic mapping and one for localizing MT/MST and recording neural responses to the plaid stimuli. Prior to scanning participants were familiarized with the stimuli and task first in the laboratory and then in a mock scanner located at the Unité de Neuroimagerie Fonctionnelle (UNF), Institut Universitaire de Gériatrie de Montréal (University of Montreal). Eye movements were recorded during the laboratory sessions using a Quick Glance 1 eye tracking system (EyeTech Digital Systems, USA) to ensure that participants were able to maintain stable fixation with both their amblyopic and non-amblyopic eye under monocular viewing conditions. We were also careful to ensure that the percept of pattern or component motion for each of the three plaid stimuli remained stable for the 16 second presentation time used during scanning and did not differ between the amblyopic and non-amblyopic eyes for any of the amblyopic participants tested. Within the mock scanner, observers viewed the plaid stimuli and held down one response button to report coherent motion and another to report incoherent motion. Therefore, if the percept changed during the 16 second presentation interval the participant could simply release one button and depress the other to indicate the switch (Hupe and Rubin, 2003; Thompson et al., 2008). The same procedure was used during scanning to control attention and monitor the way in which the plaids were being perceived. No perceptual switches were reported at any point during the study and all observers reported the coherent plaids as moving coherently and the incoherent plaid as moving incoherently under all viewing conditions. The fact that there was no difference in the perception of these plaid stimuli between the amblyopic and non-amblyopic eyes is consistent with previous psychophysical work (Thompson et al., 2008).

Scanning was performed at the Unité de Neuroimagerie Fonctionnelle (UNF), Institut Universitaire de Gériatrie de Montréal (Université de Montréal) using a Siemens 3T whole-body TRIO system (Erlangen, Germany) with an eight-channel receive-only head coil. Each scanning session began with the acquisition of a high resolution three dimensional T1 weighted image which was acquired using an MPRAGE sequence (TR = 2300 ms; TE = 2.94 ms; flip angle = 9°, 176 slices, voxel size = $1 \times 1 \times 1$ mm^3). Ten functional scans were then conducted; six for the plaid stimuli (three scans per eye) and four for hMT+ localization/subdivision stimuli (two scans per eye). The sequence of scans was randomized across participants. All functional scans consisted of 148 T2*-weighted gradient-echo echoplanar images depicting blood oxygen level-dependant (BOLD) contrast (Ogawa et al., 1990) (TR = 2000 ms, TE = 30 ms, flip angle = 90°, in plane resolution = 3×3mm and slice thickness = 3 mm) acquired in each of 27 planes. The slices were oriented parallel to the calcarine sulcus and arranged to include the pulvinar.

Data analysis

Analysis of the plaid and hMT+ localization data was conducted using the commercially available BrainVoyagerQX fMRI analysis software package. Functional scans were high-pass filtered and motion corrected using sub-routines within BrainVoyager and aligned to the high resolution anatomical scan. Functional and anatomical data were then transformed into Talairach space (Talairach and Tournoux, 1988) to allow for a direct comparison of region of interest locations with previous studies.

hMT+ was defined using a general linear model analysis of the four scanning runs during which participants viewed the RDK stimulus. This allowed for t-statistic maps representing a contrast between the full-field dynamic RDK condition and the static RDK condition to be visualized on inflated representations of the cerebral hemispheres at a false discovery rate (FDR) corrected level of $p<0.001$ (Benjamini and Hockberg, 1995). hMT+ was defined as a stimulus responsive region in the appropriate anatomical location (Dumoulin et al., 2000; Ptito et al., 2003; Tootell and Taylor, 1995; Tootell et al., 1995a,b). In order to subdivide hMT+ into MT and MST, the t-statistic maps (FDR corrected at $p<0.001$) representing the contrast between hemifield stimulation and the static RDK condition were visualized on the inflated representation of the cerebral hemisphere ipsilateral to the stimulated hemifield. MST was defined as the area within the larger hMT+ region of interest (ROI) that responded to ipsilateral hemifield stimulation and MT was defined as the area of hMT+ that responded to contralateral stimulation once MST had been removed (Desimone and Ungerleider, 1986; Duffy and Wurtz, 1991; Dukelow et al., 2001; Huk et al., 2002; Komatsu and Wurtz, 1988; Raiguel et al., 1997; Smith et al., 2006).

ROIs for V1, V2, V3 *(V3d)*, V3a, VP *(V3v)* and V4v were generated by an automated volumetric analysis of the retinotopic mapping data (Barnes et al., 2010; Dumoulin et al., 2003). The ROIs were then converted to BrainVoyager format using custom Matlab software. Regions of interest for the pulvinar were defined anatomically based on previous reports (Kastner et al., 2004; Ptito et al., 1999; Villeneuve et al., 2005). To ensure that all voxels with the retinotopic ROIs and the pulvinar ROIs were responsive to visual stimulation within the area of the visual field covered by the plaid stimuli, a general linear model analysis was conducted on the plaid stimulus scans for each participant. This allowed for a contrast between the blank fixation condition and all other conditions (i.e. the three dynamic plaids and the static plaid). Only voxels that responded significantly at a FDR correction of $q<0.001$ were included in the ROIs.

Raw time series data from all of the plaid stimulus scanning runs were extracted from every ROI for both hemispheres for each participant. Time series data for each plaid condition were normalized to the directly preceding 2 TRs (at the end of the blank fixation condition) to provide a baseline for the %BOLD change measure. Average %BOLD change was then calculated as the mean of the %BOLD change values within an 8 TR (16 s) window starting 3 TRs (6 s) after stimulus onset and ending 3 TRs after stimulus offset to account for the hemodynamic delay.

Results

Psychophysical measures

Behavioral data collected during scanning indicated that observers did not experience any bi-stability for any of the plaid stimuli. In addition, coherent plaids always resulted in coherent motion percepts and incoherent plaids always resulted in incoherent motion percepts. In agreement with our previous study (Thompson et al., 2008), these psychophysical measures did not differ between amblyopic and non-amblyopic eyes.

Plaid responses within the extra-striate cortex

Extra-striate visual areas were classified as being differentially activated by coherent motion and incoherent motion if their response to the incoherent motion stimulus was significantly different from their response to each of the two coherent motion stimuli (Villeneuve et al., 2005). This ensured that any activation differences could not be explained by the spatial frequency content of the stimuli. To test for these differences, a within subjects ANOVA was conducted for each visual area for each viewing condition with a single factor of plaid type (0.2 cpd coherent motion vs. 0.5 cpd coherent motion vs. incoherent motion). An FDR correction, as implemented by Benjamini and Hockberg (1995), was used to control for multiple

comparisons at this level of the analysis. If a significant main effect of plaid type was present, post-hoc paired t-tests were then conducted to ensure that the incoherent motion stimulus was significantly different from both coherent motion stimuli. Statistical values for this analysis are reported in Table 2. The degrees of freedom of all ANOVAs were corrected for sphericity using the Huhn-Feldt correction where necessary.

The results for hMT+ are shown in Fig. 2. For the control participants, this area was differentially activated by coherent motion and incoherent motion, with the response to incoherent motion being significantly stronger than the response to either coherent motion stimulus (Table 2). Differential activation of hMT+ by coherent and incoherent motion also occurred for non-amblyopic eye viewing. This was not the case for amblyopic eye viewing however, whereby hMT+ was not differentially activated by coherent vs. incoherent plaid motion. In order to compare the response of hMT+ to the plaid stimuli viewed by the amblyopic vs. non-amblyopic eye, we conducted an ANOVA with factors of eye (amblyopic vs. non-amblyopic) and plaid type. The response of hMT+ was significantly weaker for amblyopic vs. non-amblyopic eye viewing $F(1,5)=7.1$, $p=0.045$. Post-hoc pairwise t-tests revealed that hMT+ had a significantly weaker response to the component motion stimulus for amblyopic eye viewing relative to non-amblyopic eye viewing $t(5)=2.8$, $p=0.04$, whereas the response did not differ significantly between the two eyes for either of the coherent motion stimuli; 0.2 cpd $t(5)=1.3$, $p=0.25$, 0.5 cpd $t(5)=2.3$, $p=0.067$. This suggests that the difference in hMT+ activation for amblyopic vs. non-amblyopic eye viewing was driven primarily by a relative reduction in the response to component motion under amblyopic eye viewing conditions.

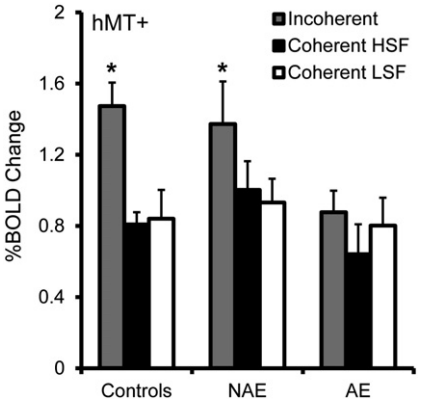

Fig. 2. The mean response of area hMT+ to coherent and incoherent motion for control observers, non-amblyopic eye viewing (NAE) and amblyopic eye viewing (AE). * indicates that the response to the incoherent motion stimulus was significantly different from the response to both coherent motion stimuli (see Table 2), HSF = high spatial frequency (0.5 cpd), LSF = low spatial frequency (0.2 cpd). Error bars in all figures indicate between subjects SEM.

To assess whether this difference in the response of hMT+ to plaid stimuli for amblyopic vs. non-amblyopic eye viewing was related to any clinical factors, we quantified the difference in hMT+ activation for coherent vs. incoherent plaid stimuli for the amblyopic eye of each participant. This was done by subtracting the mean of the %BOLD change for the two coherent stimuli from the %BOLD change for the incoherent stimulus. We did not find any correlations between amblyopic eye acuity or the angle of strabismus and coherent motion selectivity in hMT+ for amblyopic eye viewing. However, when we split our group of amblyopic observers into those who had been patched in childhood (AS, ML and VD) and those who had not (AR, GN, RD), we found that those patients with a history of patching showed significantly greater hMT+ BOLD activation for the incoherent vs. coherent plaid stimuli than those who had not been patched, $t(4)=3.0$, $p=0.04$. In other words, the patients who had been patched showed responses in hMT+ for amblyopic eye viewing that were more similar to non-amblyopic eye viewing and control observer responses. It is important to note, however, that while being suggestive, this analysis did not survive an FDR correction for all possible comparisons between the BOLD response and clinical factors.

We were able to subdivide hMT+ into MT and MST in four hemispheres across three of our amblyopic observers (AS both hemispheres; AR and RD left hemisphere only). Although these data were only available from a limited number of participants, they do indicate that both MT and MST contributed to the abnormal amblyopic eye responses found for hMT+ (Fig. 3).

For the control participants, all extra-striate visual areas were differentially activated by coherent motion and incoherent motion (Fig. 4). Only hMT+ showed this response for non-amblyopic eye viewing (Fig. 4), although it is evident from Fig. 4 that the general trend of responses in extra-striate visual areas was comparable to the control data (i.e. stronger responses to the incoherent motion stimulus than to the coherent motion stimuli). For amblyopic eye viewing (Fig. 4), only ventral stream area VP showed significant differential activation in response to coherent vs. incoherent motion, although trends were evident in V2 and V3a. A series of ANOVAs with factors of eye and plaid type were conducted for each extrastriate region to assess the relative response of each area to amblyopic vs. non-amblyopic eye viewing conditions. Significant differences between the two eyes were found at V2; $F(1,5)=16.6$, $p=0.01$, V3; $F(1,5)=9.0$, $p=0.03$ and V3a; $F(1,5)=14.8$, $p=0.012$, indicating a general attenuation of the response of these regions to amblyopic eye input. Conversely, no significant difference between amblyopic

Table 2
Results of the statistical tests used to identify whether a particular visual area was differentially activated by incoherent vs. coherent motion. The symbol * in the eye column indicates that a condition meets the requirements for being able to make this discrimination. NS = non-significant, LSF = low spatial frequency (0.2 cpd), HSF = high spatial frequency (0.5 cpd). See Plaid responses within the extra-striate cortex for further details.

Area	Eye	ANOVA (FDR corrected)	LSF coherent vs. incoherent	HSF coherent vs. incoherent
hMT+	Control*	$F(2,12)=18.8$, $p<.001$	$t(6)=6.0$, $p<.001$	$t(6)=6.0$, $p=.002$
	Non-amblyopic*	$F(2,6)=8.2$, $p=.03$	$t(5)=2.7$, $p=.04$	$t(5)=4.2$, $p=.009$
	Amblyopic	$F(2,10)=2.1$, $p=.2$ NS	–	–
V2	Control*	$F(2,11)=12.5$, $p=.002$	$t(6)=4.5$, $p=.008$	$t(6)=3.9$, $p=.004$
	Non-amblyopic	$F(2,9)=2.7$, $p=.1$ NS	–	–
	Amblyopic	$F(2,9)=3.2$, $p=.09$ NS	–	–
V3	Control*	$F(2,9)=16.4$, $p<.001$	$t(6)=4.0$, $p=.007$	$t(6)=7.4$, $p<.001$
	Non-amblyopic	$F(1,5)=4.1$, $p=.1$ NS	–	–
	Amblyopic	$F(1,7)=4.5$, $p=.03$	$t(5)=4.1$, $p=.009$	$t(5)=1.7$, $p=.1$ NS
VP	Control*	$F(2,12)=16.2$, $p<.001$	$t(6)=5.0$, $p=.003$	$t(6)=3.3$, $p=.02$
	Non-amblyopic	$F(2,10)=2.6$, $p=.1$ NS	–	–
	Amblyopic*	$F(2,10)=7.7$, $p=.01$	$t(5)=3.3$, $p=.02$	$t(5)=3.2$, $p=.02$
V3a	Control*	$F(2,12)=17.1$, $p<.001$	$t(6)=4.4$, $p=.005$	$t(6)=4.9$, $p=.003$
	Non-amblyopic	$F(2,7)=4.5$, $p=.06$ NS	–	–
	Amblyopic	$F(2,10)=2.0$, $p=.2$ NS	–	–
V4	Control*	$F(2,11)=14.2$, $p=.001$	$t(6)=4.3$, $p=.005$	$t(6)=4.0$, $p=.007$
	Non-amblyopic	$F(2,6)=2.0$, $p=.2$ NS	–	–
	Amblyopic	$F(2,10)=4.7$, $p=.04$ NS	–	–

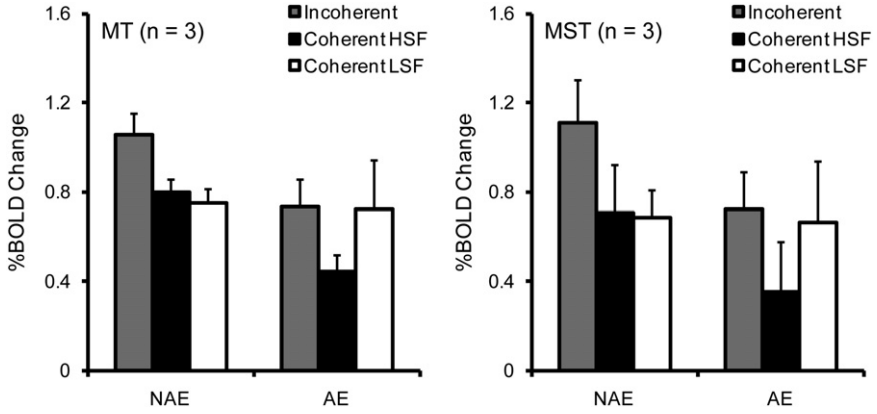

Fig. 3. The responses from the MT and MST subregions within the larger hMT+ complex for three participants with amblyopia. Both areas show a similar pattern of results as hMT+ (see Fig. 2) when driven by the non-amblyopic eye (NAE) vs. the amblyopic eye (AE), HSF = high spatial frequency (0.5 cpd), LSF = low spatial frequency (0.2 cpd).

and non-amblyopic viewing was found for VP; $F(1,5) = 1.3$, $p = 0.3$ or V4; $F(1,5) = 3.3$, $p = 0.13$, which suggests a possible preservation of the response of these regions to amblyopic eye viewing of plaid stimuli.

Primary visual cortex and the pulvinar

In addition to extra-striate visual areas, we also recorded responses from the primary visual cortex (V1) and the pulvinar. The response of V1 was significantly attenuated in observers with amblyopia compared to controls, $F(1,5) = 7.9$, $p = 0.037$ (Fig. 5, left panel). However the relative response of V1 to the plaid stimuli was consistent across both eyes of amblyopes and controls, whereby stronger responses were found for the two plaid stimuli with higher spatial frequency components (i.e. the incoherent stimulus and the high spatial frequency coherent motion stimulus). Importantly, V1 did not reliably discriminate between coherent and incoherent motion for amblyopes or controls (Fig. 5).

We were able to identify reliable pulvinar activation in four of the observers with amblyopia (AR, AS, RD, VD) and all seven controls. For controls, the pulvinar was differentially activated by coherent and incoherent motion (Fig. 5, right panel). For the amblyopic observers, the pulvinar did not reliably discriminate between coherent and incoherent motion, however as can be seen in Fig. 5, the data showed an appropriate trend. A within subjects ANOVA with factors of eye (amblyopic vs. non-amblyopic) and plaid type revealed that the response of the pulvinar differed significantly between the two eyes of the observers with amblyopia, $F(1,3) = 15.4$, $p = 0.03$. Post hoc paired t-tests revealed that the difference between the two eyes was driven by a significant reduction in the response of the pulvinar to the high spatial frequency coherent plaid under amblyopic eye viewing conditions, $t(3) = 3.4$, $p = 0.04$. The response to the low spatial frequency plaid did not differ significantly between the two eyes, although it was weaker under amblyopic eye viewing conditions $t(3) = 1.0$, $p = 0.4$. Interestingly however, the response of the pulvinar to the incoherent motion stimulus was very similar between the two eyes $t(3) = -0.1$, $p = 0.9$. In fact for 3 out of 4 of the observers with amblyopia, the response of the pulvinar to the incoherent stimulus was stronger for the amblyopic eye than for the non-amblyopic eye (AR, AS and VD).

Discussion

This study was designed to test the hypothesis that the unexpectedly normal perception of plaid stimuli by amblyopic eyes that has previously been demonstrated (Thompson et al., 2008) is mediated by a network of neural areas that is distinct from those supporting plaid perception for non-amblyopic eyes. We found that hMT+ (and both MT and MST sub-regions in a subset of patients) did not respond differentially to coherent vs. incoherent motion for amblyopic eye viewing even though the amblyopic eye perceived both types of motion normally. This was not the case for control eye viewing or non-amblyopic eye viewing, whereby hMT+ had a significantly stronger response to incoherent vs. coherent motion in accordance with previous human neuroimaging studies (Castelo-Branco et al.,

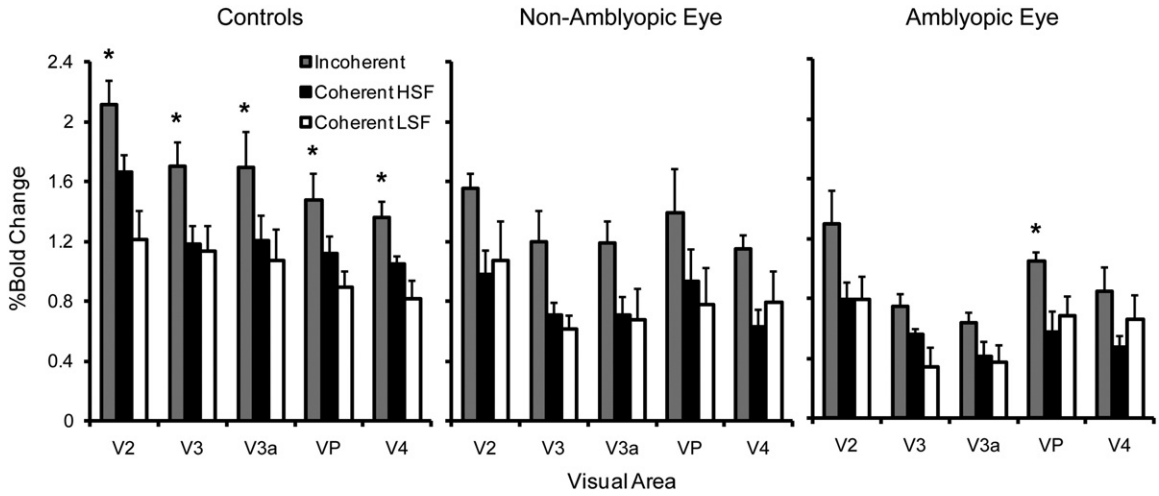

Fig. 4. The response of extra-striate visual areas to coherent and incoherent motion. * indicates that the response to incoherent motion is significantly different from both coherent motion stimuli (see Table 2).

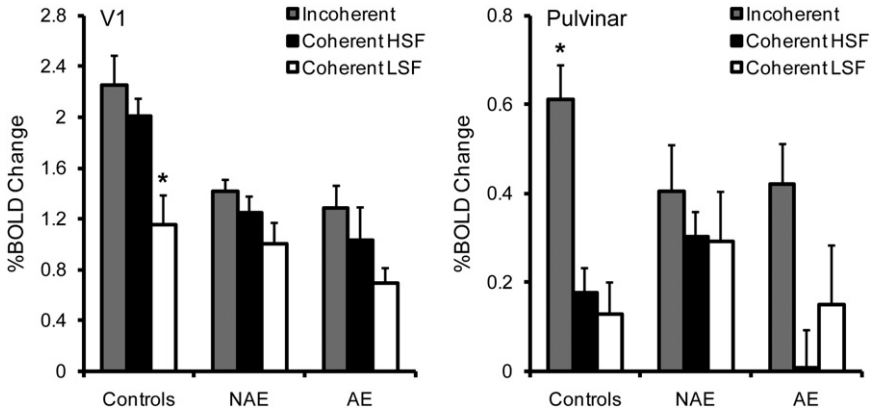

Fig. 5. The mean response of V1 (left panel) and the pulvinar (right panel, n = 4 for amblyopes) to coherent and incoherent motion for controls (n = 6), non-amlyopic eye viewing (NAE) and amblyopic eye viewing (AE). * indicates that a condition is significantly different from the other two. V1: $F(2,12) = 22.6$, $p < .001$; coherent LSF vs. coherent HSF, $t(6) = 4.9$, $p = 0.003$; coherent LSF vs. incoherent, $t(6) = 6.0$, $p = 0.001$. Pulvinar: $F(2,12) = 14.4$, $p = .001$; coherent HSF vs. incoherent, $t(6) = 4.3$, $p = .005$; coherent LSF vs. incoherent, $t(6) = 4.7$, $p = .003$.

2002; Villeneuve et al., 2005). A detailed analysis of the hMT+ responses indicated that the most pronounced difference in hMT+ function between amblyopic eye viewing vs. non-amblyopic eye viewing was a relative reduction in the response to incoherent motion stimuli.

The dissociation between normal perception and abnormal patterns of neural activity that was present in our data for amblyopic eye viewing raises the interesting possibility that the visual system of these patients was able to partially compensate for hMT+ deficits by recruiting an alternate neural network for plaid perception. This idea is consistent with the current literature on psychophysical measurements of motion perception in adults with amblyopia. As described in the Introduction, motion coherence thresholds measured using random dot kinematograms are elevated in observers with amblyopia (Simmers et al., 2003, 2006). In addition, amblyopic observers exhibit elevated Dmax thresholds (Ho and Giaschi, 2006) and a poorer signal to noise ratio when pooling motion information (Thompson et al., 2011). In contrast, amblyopic observers have been found to be relatively unaffected in their performance of psychophysical tasks that do not emphasize the segregation of signal motion from noise. These include motion detection and direction discrimination (Hess and Anderson, 1993; Hess et al., 1978), integration of local motion (Hess et al., 2006) and biological motion perception in the absence of noise (Thompson et al., 2007). A comparable pattern of motion perception deficits has been reported in Macaque monkeys secondary to lesions of MT/MST. Initially, these lesions result in pronounced deficits for a wide range of motion tasks, however, after training, performance on motion tasks that do not include noise can recover to normal levels. Conversely, the performance of tasks including noise, such as judgements involving RDKs, remains impaired (Pasternak and Merigan, 1994; Rudolph and Pasternak, 1999). Presumably this partial recovery of visual function is due to the recruitment of an alternative neural network for motion processing that is capable of supporting some aspects of motion perception but not the segregation of motion signals from noise. It is our conjecture that a similar compensatory network may be in operation for patients with amblyopia. In this context we were interested to find preliminary evidence that the patients who had been treated with patching may show more normal responses within hMT+ than those who had not. This raises the possibility that the enforced use of the amblyopic eye associated with patching may promote more normal development of extrastriate visual areas in patients with amblyopia.

Our results point towards two candidate regions that may contribute to the compensatory network we propose. These are ventral V3 and the pulvinar. Ventral V3 was differentially activated by coherent vs. incoherent motion for amblyopic eye viewing but not for non-amblyopic viewing. In addition the overall response of this area was not significantly reduced under amblyopic viewing conditions. The importance of ventral V3 in human plaid perception has been demonstrated previously (Wenderoth et al., 1999). It has also previously been demonstrated that the pulvinar is capable of discriminating between incoherent and coherent motion both in animals (Merabet et al., 1998) and humans (Villeneuve et al., 2005). While we were only able to record activity in the pulvinar of four of our participants with amblyopia, the data indicate that while the response of the pulvinar to coherent motion is relatively diminished for amblyopic eye viewing, particularly for high spatial frequencies, the response to incoherent motion remains robust. In fact, this response was stronger for amblyopic viewing than non-amblyopic viewing for three out of four participants. Although our data is necessarily limited due to the small number of participants for whom pulvinar activity could be recorded, it raises the possibility that recruitment of the pulvinar may have helped compensate for the loss of response to incoherent motion that we identified in hMT+ for the same participants.

Two previous studies have explicitly investigated the response of area hMT+ to dynamic stimuli in humans with amblyopia and both have reported reduced activity in hMT+ in response to either dynamic concentric squarewave gratings (Bonhomme et al., 2006) or RDKs (Ho and Giaschi, 2009). Our finding of an overall reduction in the response of hMT+ to dynamic plaid stimuli when driven by the amblyopic eye is in agreement with these previous studies and, as a whole, these fMRI data indicate a loss of function within this cortical area. A recent neurophysiological study of MT neurons has also found evidence for abnormal MT function in amblyopia. El-Shamayleh et al. (2011) found that fewer cells in MT were responsive to amblyopic eye stimulation vs. non-amblyopic eye stimulation in macaque monkeys made experimentally amblyopic. This supports previous studies in the cat (Schroder et al., 2002; Sireteanu and Best, 1992). In addition, cells driven by the amblyopic eye were found to be less direction selective and less tolerant of noise. Extending previous findings, our current data provides preliminary evidence that the motion processing deficits we observed in hMT+ for amblyopic eye viewing were present in both MT and MST. However it should be noted that this observation was based on only a subset of our observers with amblyopia (n = 3).

For control participants we found that all extra-striate areas were differentially activated by coherent vs. incoherent motion as has previously been reported (Castelo-Branco et al., 2002; Huk and Heeger, 2002). The observers with amblyopia did not show such distributed plaid motion specific responses within the extrastriate cortex. Specifically, the non-amblyopic-eye generated reliable coherent vs. incoherent motion responses only in area hMT+, whereas the amblyopic eye

generated such responses only in ventral V3. Motion processing deficits have been reported for both amblyopic and non-amblyopic viewing relative to controls (Aaen-Stockdale et al., 2007; Ho et al., 2005; Kiorpes et al., 2006) and our data raise the possibility that these deficits may reflect impoverished motion processing throughout the extrastriate visual cortex.

In context of the few fMRI studies of human amblyopia published to date, it seems that the recruitment of different brain areas to support amblyopic eye function may be limited to the dorsal motion pathway that was targeted in the current study. For example, while amblyopic eye stimulation results in significantly weaker cortical responses, the boundaries of the various topographically mapped visual areas are similar (Li et al., 2007), the cortical mapping of spatial frequency is similar (Hess et al., 2009) and the mapping of color/achromatic contrast to ventral and dorsal extrastriate pathways respectively is also similar (Hess et al., 2010) for amblyopes and controls. This indicates a functional deficit without the recruitment of distinct neural networks. In other words, similar brain areas are recruited under amblyopic and non-amblyopic eye viewing, however the response to amblyopic viewing is impoverished. This is in agreement with psychophysical deficits in spatial vision that are associated with amblyopia (e.g. Hess and Howell, 1977).

Overall, our results indicate that while patients with amblyopia are able to perceive incoherent and coherent plaid motion normally, this perception is mediated by a network of neural areas that does not emphasize hMT+, a region centrally involved in plaid perception for non-amblyopic eyes. We therefore propose that the amblyopic visual system is able to partially compensate for deficits in hMT+ function by recruiting alternative neural regions to support motion perception. On the basis of our current findings we tentatively propose V3 and the pulvinar as candidate regions. While this study is limited by the small sample size ($n = 6$), the results are the first to indicate the presence of compensatory neural mechanisms in amblyopia and as such, provide a foundation for ongoing tests of this novel hypothesis.

Acknowledgments

This work was supported by the CIHR grants MOP-14825 to CC and MOP-53346 to RFH and a FRSQ reseau en santé de la vision grant to CC and RFH.

References

Aaen-Stockdale, C., Hess, R.F., 2008. The amblyopic deficit for global motion is spatial scale invariant. Vis. Res. 48, 1965–1971.
Aaen-Stockdale, C., Ledgeway, T., Hess, R.F., 2007. Second-order optic flow deficits in amblyopia. Invest. Ophthalmol. Vis. Sci. 48, 5532–5538.
Adelson, E.H., Movshon, J.A., 1982. Phenomenal coherence of moving visual patterns. Nature 300, 523–525.
Asper, L., Crewther, D., Crewther, S.G., 2000. Strabismic amblyopia. Part 1. Psychophysics. Clin. Exp. Optom. 83, 49–58.
Barnes, G.R., Hess, R.F., Dumoulin, S.O., Achtman, R.L., Pike, G.B., 2001. The cortical deficit in humans with strabismic amblyopia. J. Physiol. (Lond) 533, 281–297.
Barnes, G.R., Li, X., Thompson, B., Singh, K.D., Dumoulin, S.O., Hess, R.F., 2010. Decreased gray matter concentration in the lateral geniculate nuclei in human amblyopes. Invest. Ophthalmol. Vis. Sci. 51, 1432–1438.
Barrett, B.T., Bradley, A., McGraw, P.V., 2004. Understanding the neural basis of amblyopia. Neuroscientist 10, 106–117.
Benjamini, Y., Hockberg, Y., 1995. Controlling the false discovery rate: a practical and powerful approach to multiple testing. J. R. Stat. Soc. B Methodol. 57, 289–300.
Bonhomme, G.R., Liu, G.T., Miki, A., Francis, E., Dobre, M.C., Modestino, E.J., Aleman, D.O., Haselgrove, J.C., 2006. Decreased cortical activation in response to a motion stimulus in anisometropic amblyopic eyes using functional magnetic resonance imaging. J. AAPOS 10, 540–546.
Born, R.T., Bradley, D.C., 2005. Structure and function of visual area MT. Annu. Rev. Neurosci. 28, 157–189.
Castelo-Branco, M., Formisano, E., Backes, W., Zanella, F., Neuenschwander, S., Singer, W., Goebel, R., 2002. Activity patterns in human motion-sensitive areas depend on the interpretation of global motion. Proc. Natl. Acad. Sci. U. S. A. 99, 13914–13919.
Clifford, C.W., Vaina, L.M., 1999. Anomalous perception of coherence and transparency in moving plaid patterns. Brain Res. Cogn. Brain Res. 8, 345–353.
Constantinescu, T., Schmidt, L., Watson, R., Hess, R.F., 2005. A residual deficit for global motion processing after acuity recovery in deprivation amblyopia. Invest. Ophthalmol. Vis. Sci. 46, 3008–3012.
Desimone, R., Ungerleider, L.G., 1986. Multiple visual areas in the caudal superior temporal sulcus of the macaque. J. Comp. Neurol. 248, 164–189.
Duffy, C.J., Wurtz, R.H., 1991. Sensitivity of MST neurons to optic flow stimuli. I. A continuum of response selectivity to large-field stimuli. J. Neurophysiol. 65, 1329–1345.
Dukelow, S.P., DeSouza, J.F., Culham, J.C., van den Berg, A.V., Menon, R.S., Vilis, T., 2001. Distinguishing subregions of the human MT+ complex using visual fields and pursuit eye movements. J. Neurophysiol. 86, 1991–2000.
Dumoulin, S.O., Bittar, R.G., Kabani, N.J., Baker Jr., C.L., Le Goualher, G., Bruce Pike, G., Evans, A.C., 2000. A new anatomical landmark for reliable identification of human area V5/MT: a quantitative analysis of sulcal patterning. Cereb. Cortex 10, 454–463.
Dumoulin, S.O., Hoge, R.D., Baker Jr., C.L., Hess, R.F., Achtman, R.L., Evans, A.C., 2003. Automatic volumetric segmentation of human visual retinotopic cortex. NeuroImage 18, 576–587.
Ellemberg, D., Lewis, T.L., Maurer, D., Brar, S., Brent, H.P., 2002. Better perception of global motion after monocular than after binocular deprivation. Vis. Res. 42, 169–179.
El-Shamayleh, Y., Kiorpes, L., Kohn, A., Movshon, J.A., 2011. Visual motion processing by neurons in area MT of macaque monkeys with experimental amblyopia. J. Neurosci. 30, 12198–12209.
Gegenfurtner, K.R., Kiper, D.C., Levitt, J.B., 1997. Functional properties of neurons in macaque area V3. J. Neurophysiol. 77, 1906–1923.
Guo, K., Benson, P.J., Blakemore, C., 2004. Pattern motion is present in V1 of awake but not anaesthetized monkeys. Eur. J. Neurosci. 19, 1055–1066.
Hess, R.F., Anderson, S.J., 1993. Motion sensitivity and spatial undersampling in amblyopia. Vis. Res. 33, 881–896.
Hess, R.F., Howell, E.R., 1977. The threshold contrast sensitivity function in strabismic amblyopia: evidence for a two type classification. Vis. Res. 17, 1049–1055.
Hess, R.F., Howell, E.R., Kitchin, J.E., 1978. On the relationship between pattern and movement perception in strabismic amblyopia. Vis. Res. 18, 375–377.
Hess, R.F., Mansouri, B., Dakin, S.C., Allen, H., 2006. Integration of local motion is normal in amblyopia. J. Opt. Soc. Am. A 23, 1–8.
Hess, R.F., Li, X., Mansouri, B., Thompson, B., Hansen, B.C., 2009. Selectivity as well as sensitivity loss characterizes the cortical spatial frequency deficit in amblyopia. Hum. Brain Mapp. 30, 4054–4069.
Hess, R.F., Thompson, B., Gole, G.A., Mullen, K.T., 2010. The amblyopic deficit and its relationship to geniculo-cortical processing streams. J. Neurophysiol. 104, 475–483.
Ho, C.S., Giaschi, D.E., 2006. Deficient maximum motion displacement in amblyopia. Vis. Res. 46, 4595–4603.
Ho, C.S., Giaschi, D.E., 2009. Low- and high-level motion perception deficits in anisometropic and strabismic amblyopia: evidence from fMRI. Vis. Res. 49, 2891–2901.
Ho, C.S., Giaschi, D.E., Boden, C., Dougherty, R., Cline, R., Lyons, C., 2005. Deficient motion perception in the fellow eye of amblyopic children. Vis. Res. 45, 1615–1627.
Hubel, D.H., Wiesel, T.N., 1965. Binocular interaction in striate cortex of kittens reared with artificial squint. J. Neurophysiol. 28, 1041.
Hubel, D.H., Wiesel, T.N., 1970. Period of susceptibility to physiological effects of unilateral Eye closure in kittens. J. Physiol. Lond. 206, 419.
Huk, A.C., Heeger, D.J., 2002. Pattern-motion responses in human visual cortex. Nat. Neurosci. 5, 72–75.
Huk, A.C., Dougherty, R.F., Heeger, D.J., 2002. Retinotopy and functional subdivision of human areas MT and MST. J. Neurosci. 22, 7195–7205.
Hupe, J.M., Rubin, N., 2003. The dynamics of bi-stable alternation in ambiguous motion displays: a fresh look at plaids. Vis. Res. 43, 531–548.
Kastner, S., O'Connor, D.H., Fukui, M.M., Fehd, H.M., Herwig, U., Pinsk, M.A., 2004. Functional imaging of the human lateral geniculate nucleus and pulvinar. J. Neurophysiol. 91, 438–448.
Kiorpes, L., McKee, S.P., 1999. Neural mechanisms underlying amblyopia. Curr. Opin. Neurobiol. 9, 480–486.
Kiorpes, L., Tang, C., Movshon, J.A., 2006. Sensitivity to visual motion in amblyopic macaque monkeys. Vis. Neurosci. 23, 247–256.
Komatsu, H., Wurtz, R.H., 1988. Relation of cortical areas MT and MST to pursuit eye movements. I. Localization and visual properties of neurons. J. Neurophysiol. 60, 580–603.
Li, X., Dumoulin, S.O., Mansouri, B., Hess, R.F., 2007. The fidelity of the cortical retinotopic map in human amblyopia. Eur. J. Neurosci. 25, 1265–1277.
Li, X., Mullen, K.T., Thompson, B., Hess, R.F., 2011. Effective connectivity anomalies in human amblyopia. NeuroImage 54, 505–516.
Majaj, N.J., Carandini, M., Movshon, J.A., 2007. Motion integration by neurons in macaque MT is local, not global. J. Neurosci. 27, 366–370.
Mansouri, B., Hess, R.F., 2006. The global processing deficit in amblyopia involves noise segregation. Vis. Res. 46, 4104–4117.
Merabet, L., Desautels, A., Minville, K., Casanova, C., 1998. Motion integration in a thalamic visual nucleus. Nature 396, 265–268.
Movshon, J.A., Adelson, E.H., Gizzi, M.S., Newsome, W.T., 1985. The analysis of moving visual patterns. Pontificiae academiae scientiarum scripta varta, pp. 117–151.
Newsome, W.T., Pare, E.B., 1988. A selective impairment of motion perception following lesions of the middle temporal visual area (MT). J. Neurosci. 8, 2201–2211.
Ogawa, S., Lee, T.M., Kay, A.R., Tank, D.W., 1990. Brain magnetic resonance imaging with contrast dependent on blood oxygenation. Proc. Natl. Acad. Sci. U. S. A. 87, 9868–9872.
Pack, C.C., Berezovskii, V.K., Born, R.T., 2001. Dynamic properties of neurons in cortical area MT in alert and anaesthetized macaque monkeys. Nature 414, 905–908.

Pasternak, T., Merigan, W.H., 1994. Motion perception following lesions of the superior temporal sulcus in the monkey. Cereb. Cortex 4, 247–259.
Ptito, M., Johannsen, P., Faubert, J., Gjedde, A., 1999. Activation of human extrageniculostriate pathways after damage to area V1. NeuroImage 9, 97–107.
Ptito, M., Faubert, J., Gjedde, A., Kupers, R., 2003. Separate neural pathways for contour and biological-motion cues in motion-defined animal shapes. NeuroImage 19, 246–252.
Raiguel, S., Van Hulle, M.M., Xiao, D.K., Marcar, V.L., Lagae, L., Orban, G.A., 1997. Size and shape of receptive fields in the medial superior temporal area (MST) of the macaque. Neuroreport 8, 2803–2808.
Rodman, H.R., Albright, T.D., 1989. Single-unit analysis of pattern-motion selective properties in the middle temporal visual area (MT). Exp. Brain Res. 75, 53–64.
Rudolph, K., Pasternak, T., 1999. Transient and permanent deficits in motion perception after lesions of cortical areas MT and MST in the macaque monkey. Cereb. Cortex 9, 90–100.
Salzman, C.D., Britten, K.H., Newsome, W.T., 1990. Cortical microstimulation influences perceptual judgements of motion direction. Nature 346, 174–177.
Schroder, J.H., Fries, P., Roelfsema, P.R., Singer, W., Engel, A.K., 2002. Ocular dominance in extrastriate cortex of strabismic amblyopic cats. Vis. Res. 42, 29–39.
Simmers, A.J., Ledgeway, T., Hess, R.F., McGraw, P.V., 2003. Deficits to global motion processing in human amblyopia. Vis. Res. 43, 729–738.
Simmers, A.J., Ledgeway, T., Mansouri, B., Hutchinson, C.V., Hess, R.F., 2006. The extent of the dorsal extra-striate deficit in amblyopia. Vis. Res. 46, 2571–2580.
Sireteanu, R., Best, J., 1992. Squint-induced modification of visual receptive fields in the lateral suprasylvian cortex of the Cat: binocular interaction, vertical effect and anomalous correspondence. Eur. J. Neurosci. 4, 235–242.
Smith, A.T., 1992. Coherence of plaids comprising components of disparate spatial frequencies. Vis. Res. 32, 393–397.
Smith, A.T., Wall, M.B., Williams, A.L., Singh, K.D., 2006. Sensitivity to optic flow in human cortical areas MT and MST. Eur. J. Neurosci. 23, 561–569.
Stoner, G.R., Albright, T.D., 1992. Neural correlates of perceptual motion coherence. Nature 358, 412–414.
Talairach, J., Tournoux, P., 1988. Co-planar stereotactic atlas of the human brain. In: Thieme (Ed.), Stuttgart, New York.
Thompson, B., Hansen, B.C., Hess, R.F., Troje, N.F., 2007. Amblyopic perception of biological motion. J. Vis. 7 485-485.
Thompson, B., Aaen-Stockdale, C.R., Mansouri, B., Hess, R.F., 2008. Plaid perception is only subtly impaired in strabismic amblyopia. Vis. Res. 48, 1307–1314.
Thompson, B., Aaen-Stockdale, C., Koski, L., Hess, R.F., 2009. A double dissociation between striate and extrastriate visual cortex for pattern motion perception revealed using rTMS. Hum. Brain Mapp. 30, 3115–3126.
Thompson, B., Richard, A., Churan, J., Hess, R.F., Aaen-Stockdale, C., Pack, C.C., 2011. Impaired spatial and binocular summation for motion direction discrimination in strabismic amblyopia. Vis. Res. 51, 577–584.
Tootell, R.B., Taylor, J.B., 1995. Anatomical evidence for MT and additional cortical visual areas in humans. Cereb. Cortex 5, 39–55.
Tootell, R.B., Reppas, J.B., Dale, A.M., Look, R.B., Sereno, M.I., Malach, R., Brady, T.J., Rosen, B.R., 1995a. Visual motion aftereffect in human cortical area MT revealed by functional magnetic resonance imaging. Nature 375, 139–141.
Tootell, R.B., Reppas, J.B., Kwong, K.K., Malach, R., Born, R.T., Brady, T.J., Rosen, B.R., Belliveau, J.W., 1995b. Functional analysis of human MT and related visual cortical areas using magnetic resonance imaging. J. Neurosci. 15, 3215–3230.
Villeneuve, M.Y., Kupers, R., Gjedde, A., Ptito, M., Casanova, C., 2005. Pattern-motion selectivity in the human pulvinar. NeuroImage 28, 474–480.
Wenderoth, P., Watson, J.D., Egan, G.F., Tochon-Danguy, H.J., O'Keefe, G.J., 1999. Second order components of moving plaids activate extrastriate cortex: a positron emission tomography study. NeuroImage 9, 227–234.